https://ntrs.nasa.gov/search.jsp?R=19820017212 2020-03-21T07:29:14+00:00Z

General Disclaimer

One or more of the Following Statements may affect this Document

- This document has been reproduced from the best copy furnished by the organizational source. It is being released in the interest of making available as much information as possible.

- This document may contain data, which exceeds the sheet parameters. It was furnished in this condition by the organizational source and is the best copy available.

- This document may contain tone-on-tone or color graphs, charts and/or pictures, which have been reproduced in black and white.

- This document is paginated as submitted by the original source.

- Portions of this document are not fully legible due to the historical nature of some of the material. However, it is the best reproduction available from the original submission.

Produced by the NASA Center for Aerospace Information (CASI)

NASA

Technical Memorandum 83913

On the Acceleration of Ions by Interplanetary Shock Waves: I: Single Encounter Considerations

M. E. Pesses

(NASA-TM-83913) ON THE ACCELERATION OF IONS BY INTERPLANETARY SHOCK WAVES. 1: SINGLE ENCOUNTER CONSIDERATIONS (NASA) 37 p HC A03/MF A01 CSCL 03B
N82-25088
Unclas
G3/93 21226

DECEMBER 1981

MAY 1982
RECEIVED
NASA STI FACILITY
ACCESS DEPT.

National Aeronautics and
Space Administration

Goddard Space Flight Center
Greenbelt, Maryland 20771

On the Acceleration of Ions by Interplanetary Shock Waves: I Single Encounter Considerations

by

M.E. Pesses *

Laboratory for Astronomy and Solar Physics
Goddard Space Flight Center, NASA
Greenbelt, MD 20771

Department of Physics and Astronomy
University of Iowa
Iowa City, IA 52242

April 1982

* National Academy of Sciences' National Research Council Fellow

ABSTRACT

The acceleration of energetic ions in interplanetary magnetosonic fast-mode shock waves is studied via analytical modeling and numerical simulations. An analytical model that combines both the shock drift and compressional acceleration mechanisms is presented. The analytical predictions of the model are shown to be in good agreement with numerical simulation results.

I. INTRODUCTION

Observations during the past two decades at 1 AU and in deep space have established a causal relationship between the passage of interplanetary shock waves and the large enhancements of energetic proton intensity that are frequently observed around the time of shock passage [Sarris and Van Allen, 1974; Pesses et al., 1979, and references in both papers].

Axford and Reed [1963] first suggested that the above relationship is due to protons being directly accelerated in interplanetary shock waves. Since then several types of interplanetary shock acceleration mechanisms have been discussed: Compression between the shock front and upstream magnetic field irregularities [Fisk, 1971]; A gradient $|\vec{B}|$ drift at the shock front in the $\vec{V} \times \vec{B}$ electric field in the shock rest frame [Chen and Armstrong, 1972, Sarris and Van Allen, 1974; Armstrong et al., 1977]; and compression between upstream and downstream magnetic field irregularities [Fisk and Lee, 1980].

The purpose of this paper, the first of three companion papers, is: 1) to construct a model which combines the above acceleration processes and 2) to present analytical expressions for energy changes, final pitch angles, and acceleration times for particles transmitted and reflected by oblique and perpendicular magnetosonic fast-mode shocks. The model presented here is used in Paper II to calculate the differential energy spectra of ions accelerated in corotating interaction region (CIR) shock waves; and compared in Paper III to high time resolution observations of CIR accelerated protons.

II. SHOCK GEOMETRY

Observations of energetic (~ 1 MeV) proton events associated with shock waves in deep space [Pesses et al., 1979] and at 1 AU [Sarris, 1973, and references therein] show that these shocks are apparently all of the magnetosonic fast-mode variety. No observations of energetic proton events associated with either magnetosonic slow-mode or Alfven shock waves have, to my knowledge, been reported. Therefore, the acceleration model to be developed here will be for only the fast-mode shocks.

The magnetosonic fast-mode shocks to be considered move with a velocity $\vec{V}_s$ with respect to the upstream plasma rest frame. The plasma mass density upstream of the shock is ρ_1 and downstream ρ_2. The shocks are planar in the y - z plane of Figure 1. The shock front unit normal vector $\hat{n}$ is directed along the positive x-axis, and ψ_1 (ψ_2) is the acute angle between $\hat{n}$ and $\vec{B}_1$ ($\vec{B}_2$), the upstream (downstream) magnetic field vector. The hydrodynamic shock strength is $\rho_2\rho_1^{-1}$(= H) and the magnetic shock strength is $|\vec{B}_2||\vec{B}_1|^{-1}$ (= N). The motion of the magnetized solar wind in the shock rest frame results in a $\vec{V}_s \times \vec{B}$ electric field. In Figure 1 this $\vec{E}$ is parallel to negative y-axis. From the continuity of the tangential component of $\vec{E}$ across the shock front the upstream (E_{1y}) and downstream (E_{2y}) electric field-vectors are equal. In the model it is assumed that $\vec{V}_s$, $\hat{n}$, $\vec{B}_1$ and $\vec{B}_2$ do not vary with time or space.

III. SHOCK-ASSOCIATED ACCELERATION PROCESSES

A. Classification

A general classification scheme for charged particle acceleration mechanisms has been developed by Northrop [1963]. He shows that in a given reference frame the time (t) rate of change of a non-relativistic charged particle's kinetic energy (T) averaged over one particle gyroperiod, $\langle dT/dt \rangle_\omega$, is given by Equation (1)

$$\left\langle \frac{dT}{dt} \right\rangle_\omega = \overset{\mathrm{I}}{q\vec{G}\cdot\langle\vec{E}\rangle_\omega} + \overset{\mathrm{II}}{\mu \frac{\partial |\vec{B}|}{\partial t}} + O(m^2/q^2) \qquad (1)$$

In Equation (1) q is the particle charge, m is the particle mass, $\vec{G}$ is the particle guiding center velocity, $\langle\vec{E}\rangle_\omega$ is the average value, over one gyroperiod, of the electric intensity vector $\vec{E}$ at the position of the guiding center, $\vec{B}$ is the magnetic inductance vector at the position of the guiding center, μ is the magnetic moment of the particle (evaluated in the guiding center rest frame), and O means on the order of magnitude of. Term I in Equation (1) is the time rate of change of the particle energy due to work done by the electric field on the guiding center. Term II is an induction effect of a time dependent $\vec{B}$ and is the time rate of change of the particle energy due to the curl of $\vec{E}$ acting about the circular particle gyro orbit.

Shock drift acceleration is included in Term I, and compressional acceleration in Term II. Northrop [1963] notes that both betatron acceleration and the type of acceleration first discussed by Fermi [1949] are included in Term II.

B. Reference Frame Dependence

Interplanetary shock acceleration models calculate the particle energy gains in various frames: the shock rest frame, the upstream or downstream

plasma rest frames, and the null electric field frame where both the $\vec{V}_s \times \vec{B}$ and $\partial\vec{B}/\partial t$ electric fields are zero.

1. Shock Rest Frame

In the frame in which the shock is at rest the $V|\vec{B}|$ drift motion and also drifts due to changes across the shock front of the direction of $\vec{B}$ and the $\vec{E} \times \vec{B}$ drift velocity drift velocity result in a net displacement of the particle guiding center in the $\vec{V}_s \times \vec{B}$ electric field potential. This type of shock acceleration is called shock drift acceleration (previously called $\vec{V} \times \vec{B}$ acceleration).

As there is no $\partial\vec{B}/\partial t$ due to the shock's motion in this frame, there is no "induction" acceleration from the shock front. However, charged particles are also accelerated in this frame from the $\partial B/\partial t$, curl of $\vec{E}$ produced by moving magnetic field irregularities. Particles backscattered toward the shock by approaching upstream irregularities gain energy while particles backscattered toward the shock by receding downstream irregularities lose energy. The magnetic field irregularities are convected by the plasma bulk motion so the upstream irregularities are approaching faster than the downstream irregularities are receding. This divergence in the velocity of the irregularities at the shock front results in a net energy gain due to compression. (Axford et al., 1977; Bell, 1978).

2. Upstream Plasma Rest Frame

In the upstream plasma rest frame charged particles are accelerated by the curl of $\vec{E}$ induced by temporal variations in $\vec{B}$ due to both the motion of the shock front and approaching downstream magnetic field irregularities. A graphic way of looking at the acceleration of the shock front in this frame is given in Figure 2a. The energy gain is due to particles gyrovelocity having a component

which is parallel to the downstream $\vec{V} \times \vec{B}$ electric field.

3. Downstream Plasma Rest Frame

In the downstream plasma rest frame charged particles are accelerated by the curl of $\vec{E}$ introduced by temporal variations in $\vec{B}$ due to both the motion of the shock front and approaching upstream magnetic field irregularities. A graphic way of looking at the acceleration at the shock in this frame is shown in Figure 2b. The energy gain is due to the particles' gyrovelocity having a component parallel to the $\vec{V} \times \vec{B}$ electric field in the upstream region.

4. Null Electric Field Frame

In the null electric field frame (which moves parallel to the shock front in the shock rest frame with a speed $(\vec{V}_s \cdot \hat{n} \tan\psi_1 - |\vec{V}_s \times \hat{n}|)$, both $\langle\vec{E}\rangle\omega$ and $\partial\vec{B}/\partial t$ are zero at the shock front. Hence in the null electric field frame particles are accelerated solely by the electric field produced by moving magnetic field irregularities.

To summarize the above discussion, there are two basic energetic particle acceleration processes associated with fast-mode shocks: the shock drift mechanism which is present in the shock rest frame, and the "inductance" mechanism which at the shock front is present in both the upstream and downstream plasma rest frames, and which at moving magnetic field irregularities (compression) mechanism which is present in all four frames.

Several models of interplanetary shock acceleration have neglected one of the above acceleration processes. Fisk's [1971] snow plow model assumes that particles are accelerated by compression between the shock front and upstream magnetic field irregularities. This model explicitly assumes that reflected particles do not undergo shock drift acceleration, and implicitly assumes that transmitted particles gain no energy.

Both the energetic storm particle event models of Scholar and Morfill [1975] and the corotating particle event model of Palmer and Gosling [1978] assume that particles are accelerated by multiple reflections off the shock front. Both these models assume that reflected particles are shock drift accelerated but that transmitted particles undergo no energy gain.

The shock acceleration models of Sarris and Van Allen [1974], Armstrong et al. [1977] and Decker [1981] assume that in the shock rest frame both reflected and transmitted particles are shock drift accelerated. These models are basically concerned with quasi perpendicular ($\psi_1 \sim 90°$) shocks and ignore compressional acceleration which is not significant compared to shock drift acceleration at $\psi_1 \sim 90°$.

The corotating particle event model of Fisk and Lee [1980] does not negate either shock drift or compression. Their model assumes that particles, in the null electric field frame, are accelerated by compression, and thus in the shock rest frame particles are accelerated by both the shock drift and compression mechanisms.

IV. SINGLE SHOCK ENCOUNTER ANALYTICAL EXPRESSIONS

A. Post Encounter Energies

1. Choice of Coordinate Frames

The energy a particle gains from a single reflection or transmission from a shock can be calculated in any particular frame. However, to calculate the total kinetic energy a particle gains from multiple shock encounters it is necessary to include energy changes that result from the particle's being backscattered to the shock by moving magnetic field irregularities. If the expression for the particle energy gain from a single shock encounter is given in terms of the pre-encounter and post-encounter energies in the particle pre- and post-encounter plasma rest frame, then the particle backscattering, which is assumed elastic in a plasma rest frame, will result in no additional energy gains. The backscattering, compressional energy gains come from the relative velocity of the upstream and downstream plasma rest frames.

The energy gain per shock encounter (one encounter is composed of several shock crossings) is calculated using the following procedure: First, the particle velocity is transformed from the pre-encounter plasma rest frame of the particle to the null electric field frame; second, an algorithm is used to determine if the particle is reflected or transmitted by the shock and what the post-encounter pitch angle is; third, the post-encounter particle velocity is transformed into the post-encounter plasma rest frame of the particle.

It will be shown in the section on numerical simulations that in the null electric field frame the pre-encounter and post-encounter value of μ when averaged over gyrophase are equal.

In calculating the energy gains the following assumptions are made:

(1) contributions to the $\vec{B}$ field due to the interacting particles are negligible;

(2) energy losses due to electromagnetic radiation are ignorable;

(3) no collisions occur between the interacting particles;

(4) $\vec{V}_s$, H, N, and ψ_1 do not change during the particles' shock interaction, and

(5) the ions to be accelerated are well above the thermal distribution.

Previous analytical studies of the interaction of charged particles with interplanetary shock waves have been carried out by several authors for perpendicular shocks [Shabanskii, 1962; Schatzman, 1963; Pesses, 1981] and for oblique shocks [Hudson, 1965; Alekseyev and Kropotkin, 1970; Singer and Montgomery, 1971; Sarris and Van Allen, 1974; Vansl'yed et al., 1978].

In the upstream (downstream) plasma rest frame the null electric field frame must move parallel to $\vec{B}_1$ ($\vec{B}_2$), otherwise $\vec{V} \times \vec{B} \neq 0$. The null electric field frame must also move along the field lines at the rate at which the shock does, otherwise $\partial\vec{B}/\partial t \neq 0$. Hence, the null electric field frame moves with respect to either the upstream or downstream plasma rest frame parallel to the magnetic field vector with a speed equal to the projection of the shock velocity along the magnetic field lines.

The transformation from the upstream plasma rest frame to the null electric field frame is carried out by moving with a velocity $\vec{V}_1$, where

$$\vec{V}_1 = V_{1x} \sec \psi_1 \hat{B}_1 \qquad (2),$$

$V_{1x} = \vec{V}_s \cdot \hat{n}$, and $\hat{B}_1 = \vec{B}_1/|\vec{B}_1|$. The transformation from the downstream plasma rest frame to the null electric field frame is carried out by moving with a velocity $\vec{V}_2$, where

$$\vec{V}_2 = \frac{N}{H} V_{1x} \sec \psi_1 \hat{B}_2 \qquad (3),$$

and $\hat{B}_2 = \vec{B}_2/|\vec{B}_2|$.

2. Reflection and Transmission Considerations

The algorithm that determines if a particle is transmitted or reflected in the null electric field frame is derived by demanding that the pre- and post-encounter particle kinetic energy and angular momentum about the guiding center be equal. The particle angular momentum $\vec{L}$ is given by the cross product of the particle gration velocity and gyroradius,

$$\vec{L} = -\frac{\text{sign}(q)\ m^2 V_i^2 \sin^2 \alpha_i}{q|\vec{B}|^2} \vec{B} \qquad (4)$$

where $V_i(\alpha_i)$ is the particle speed (pitch angle) in the plasma rest frame of the particle. When the particle is directed towards the upstream region $0 < \alpha_i < 90°$. Numerical simulations to be discussed later show that a particle will not be reflected if it can conserve angular momentum and energy by being transmitted. If transmission would violate a conserved quantity a particle would be reflected. The condition under which incident upstream particles are transmitted downstream by the shock, and incident downstream particles are transmitted upstream by the shocks, are given by Equations (5) and (6), respectively.

$$1/2\ m\ NV_i^2 \sin^2 \alpha_i < 1/2\ m\ (|\vec{V}_1| + V_i^2 - 2|\vec{V}_1|V_i \cos \alpha_i) \qquad (5)$$

$$1/2\ m\ N^{-1}V_i^2 \sin^2 \alpha_i < 1/2\ m\ (|\vec{V}_2| + V_i^2 - 2|\vec{V}_2|V_i \cos \alpha_i) \qquad (6)$$

For particles initially upstream the pitch angle boundary $\alpha_{1,2}$ between reflected and transmitted particles for given values of V_i, $\vec{V}_1$ and N are found by equalling the right and left hand sides of (5) and solving for α. This gives:

$$\cos \alpha_1 = R\, N^{-1} \left[1 + \sqrt{(N-1)(N R^{-2} - 1)}\right] \quad (7),$$

$$\cos \alpha_2 = R\, N^{-1} \left[1 - \sqrt{(N-1)(N R^{-2} - 1)}\right] \quad (8),$$

where $R = |\vec{V}_1| V_1^{-1}$. Upstream particles with $\cos \alpha_i > R$ cannot be overtaken by the shock and so do not interact with it. Upstream particles are reflected when either $\cos^{-1} R < \alpha_i < \alpha_2$ and $R \leq 1$ or when $\alpha_1 < \alpha_i < \alpha_2$ and $R > 1$. Upstream particles are transmitted when $\alpha_i > \alpha_2$ and also when $\alpha_i < \alpha_1$ provided $R > 1$. When $R = \sqrt{N}$, $\alpha_1 = \alpha_2$ and all upstream particles are transmitted. When $R > \sqrt{N}$, the right hand sides of (7) and (8) are complex numbers; and numerical simulations show that all upstream particles are transmitted [Chen, 1975].

For particles that are initially downstream Parker [1963] has shown that they are either transmitted upstream or do not interact with the shock. No initially downstream particles are reflected. Downstream particles with $\cos \alpha_i < JR$, where $J = NH^{-1}$, cannot overtake the shock and so do not interact with it. Downstream particles with $\cos \alpha_i > JR$ are transmitted upstream.

The upstream noninteraction η_u, reflection r_u, and transmission τ_u coefficients of the shock as a function of R and N are given in Equations (9a-c) These equations are for an initial pitch angle distribution that is isotropic with respect to $\vec{B}$ in the upstream plasma rest frame.

$$\eta_u = \begin{cases} \pi^{-1} \cos^{-1} R & R \leq 1 \\ 0 & R > 1 \end{cases} \quad (9a)$$

$$r_u = \begin{cases} \pi^{-1}(\alpha_2 - \pi\, \eta_u) & R \leq 1 \\ \pi^{-1}(\alpha_2 - \alpha_1) & R > 1 \end{cases} \quad (9b)$$

$$\tau_u = 1 - r_u - \eta_u \quad (9c)$$

Some upstream particles will always be reflected by the shock provided $R < \sqrt{N}$ and $N > 1$. The downstream transmission τ_d and noninteraction η_d

coefficients of the shock as a function of JR and N are given in Equations (10a-b). These equations are for an initial pitch angle distribution that is isotropic with respect to $\vec{B}$ in the downstream plasma rest frame.

$$\tau_d = \pi^{-1}\cos^{-1}(JR) \qquad JR < 1 \tag{10a}$$

$$= 0 \qquad JR > 1$$

$$\eta_d = 1 - \tau_D \tag{10b}$$

3. Energy Change

Using the method discussed previously in section IV-A the fractional kinetic energy change, $(T_{final} - T_{initial})/T_{initial}$, per shock encounter in the plasma rest frame(s) for upstream particles reflected upstream $\Delta T_R/T_i$, upstream particles transmitted downstream $\Delta T_D/T_i$, and downstream particles transmitted upstream $\Delta T_U/T_i$, are presented in Equations (11), (12), and (13) respectively.

$$\frac{\Delta T_R}{T_i} = 4R(R - \chi) \tag{11}$$

$$\frac{\Delta T_D}{T_i} = R\{R(J^2 + 1) - 2\chi - 2J[1 + R(R - 2\chi) - N S^2]^{1/2}\} \tag{12}$$

$$\frac{\Delta T_U}{T_i} = R\{R(J^2 + 1) - 2J\chi + 2[1 + JR(JR - 2\chi) - S^2 N^{-1}]^{1/2}\} \tag{13}$$

where $\chi = \cos\alpha_i$ and $S = \sin\alpha_i$. Note that in Equations (11-13) $\Delta T/T_i$ does not $\to \infty$ as $\psi_1 > 90°$ (i.e. as $R \to \infty$). All upstream particles are transmitted when $\sec\psi_1 > V_i V_{1x}^{-1}\sqrt{N}$. Hence, $\Delta T_R/T_i$ does not approach ∞. Expanding the radical in Equation (12) and taking the limit $\psi_1 \to 90°$ gives

$$\lim_{(\psi_1 \to 90°)} \frac{\Delta T_D}{T_i} = (N - 1)S^2 \tag{14}$$

and hence $\Delta T_D/T_i$ does not approach ∞. No downstream particles are transmitted upstream when $\sec\psi_1 > V_i V_{1x}^{-1} J^{-1}$. So $\Delta T_U/T_i$ does not $\to \infty$.

Two examples of how shock drift and compressional energy gains are both included in the above equation are given below. Consider a particle that is reflected back and forth between the shock front and upstream magnetic field irregularities. The particle has an initial energy T_1 in the upstream plasma rest frame. The post-reflection energy in the upstream plasma rest frame T_2 can be calculated form Equation (11). After backscattering towards the shock particle's energy is still T_2. The energy in the upstream plasma rest frame after a second shock front reflection can be calculated from equation (11) again, and so on. Now consider a particle that is transmitted back and forth across the shock front. The particle has an initial energy T_1 in the upstream plasma rest frame. The particle's energy in the downstream plasma rest frame after it has been transmitted downstream (T_2) can be calculated from Equation (12). After backscattering toward the shock the particle's energy in the downstream plasma rest frame is still T_2. The particle's energy in the upstream plasma rest frame after being transmitted upstream (T_3) can be calculated from Equation (13). After again backscattering towards the shock of the particle energy in the upstream plasma rest frame is unchanged, and Equation (12) can be used to calculate the particle's energy in downstream plasma rest frame after it has been transmitted downstream a second time, and so on.

4. Maximum Values of $\Delta T/T_1$

The maximum value of $\Delta T/T_1$ in Equation (11) occurs for $\alpha_1 = \alpha_2$ and in Equation (13) for $\cos \alpha_1 = JR$. In Equation (12) the maximum value of $\Delta T/T_1$ occurs for $\alpha_1 = \alpha_2$ when $R \leq \sqrt{N}$ and for

$$\cos \alpha_1 = RN^{-1} \{1 - [(N - 1)(J^2 N - 1)^{-1} (1 - NR^{-2})]^{1/2} \},$$

when $R > \sqrt{N}$. The maximum values of $\Delta T/T_1$ as a function of R, N, and J are given in Equations (15) - (17).

$$\max \frac{\Delta T_R}{T_i} (R,N) = 4R^2 \frac{(N-1)}{N} \left\{1 + \left[\frac{1}{N-1} \left(\frac{N}{R^2} - 1\right)\right]^{1/2}\right\} \tag{15}$$

$$\max \frac{\Delta T_D}{T_i} (R,N,J) = R^2 \left\{J^2 + 1 - \frac{2}{N} \left\{1 - \left[(N-1)\left(\frac{N}{R^2} - 1\right)\right]^{1/2}\right\}\right\} \tag{16a}$$

$$R < \sqrt{N}$$

$$\max \frac{\Delta T_D}{T_i} (R,N,J) = R^2 \left\{J^2 + 1 - \frac{2}{N} \left\{1 + \left[(N-1)(NJ^2-1)\left(1 - \frac{N}{R^2}\right)\right]^{1/2}\right\}\right. \tag{16b}$$

$$R > \sqrt{N}$$

$$\max \frac{\Delta T_U}{T_i} (R,N,J) = R^2 (1 - J^2) + 2R \left[\left(1 - \frac{1}{N}\right)(1 - J^2R^2)\right]^{1/2} \tag{17}$$

The largest value of $\Delta T/T_i$ as a function of N and J is obtained by finding the value of R which makes the value of the equations for max $\Delta T/T_i(R,N,J)$ a maximum. The largest value of $\Delta T/T_i$ for $R < \sqrt{N}$ occurs for reflected particles and is given by Equation (18).

$$\max \frac{\Delta T}{T_i} = 2(N-1) \left\{1 + [N(N-1)^{-1}]^{1/2}\right] \qquad R < \sqrt{N} \tag{18}$$

The maximum value of $\Delta T/T_i$ for $R > \sqrt{N}$ occurs for transmitted downstream particles and is found by substituting $R^2 = 0.5\ N[1 + (1 - 4\beta)^{-1/2}]$ into Equation (16b), where

$$\beta = N^{-1}(N - 1)(NJ^2 - 1)(1 + J^2 - 2N^{-1})^{-2}.$$

The maximum value of $\Delta T/T_i$ as a function of N is, for N = 2, 4.83; for N = 3, 8.90; and for N = 4, 12.93.

B. Post Shock Pitch Angles

1. General Considerations

The equations for $\Delta T/T_i$ presented in Section IV-A3 give the particle total kinetic energy change per reflection or transmission by the shock. To calculate the post encounter pitch angle it is necessary to know both the post-encounter parallel and perpendicular kinetic energy of the particle. Northrop [1963] shows that in a given reference frame the time rate of change of a non-relativistic particle's parallel kinetic energy ($T_\parallel$) and perpendicular kinetic energy ($T_\perp$) averaged over one particle gyroperiod $\langle dT_\parallel/dt\rangle\omega$ and $\langle dT_\perp/dt\rangle\omega$, are given by Equations (19) and (20) respectively.

$$\left\langle\frac{dT_\parallel}{dt}\right\rangle\omega = qV_\parallel E_\parallel - \mu V_\parallel \frac{\partial|\vec{B}|}{\partial s} + mV_\parallel \vec{V}_E \cdot \frac{d\hat{B}}{dt} + O(m/q) \tag{19}$$

$$\left\langle\frac{dT_\perp}{dt}\right\rangle\omega = \mu \frac{\partial|\vec{B}|}{\partial t} + \mu V_\parallel \frac{\partial|\vec{B}|}{\partial s} + \mu \vec{V}_E \cdot \nabla |\vec{B}| + m\vec{V}_E \cdot \frac{d\vec{V}_E}{dt} + O(m^2/q^2) \tag{20}$$

In (18) and (19) $V_\parallel\{E_\parallel\}$ is the component of $\vec{G}$ $\{\langle\vec{E}\rangle_\omega\}$ parallel to $\vec{B}$, $\vec{V}_E$ is the $\vec{E} \times \vec{B}$ drift velocity, $\hat{B}$ is a unit vector in the direction of $\vec{B}$, and s is the distance along the $\vec{B}$ lines of force.

In the shock rest frame temporal changes in $T_\parallel$ are due to the magnetic mirror term, $\mu V_\parallel \partial|\vec{B}|/\partial s$, and the interaction of the $\vec{E} \times \vec{B}$ drift with the change in direction of $\vec{B}$ at the shock front. Time variations in $T_\perp$ in the shock rest frame are due to the magnetic mirror force plus the interaction of the $\vec{E} \times \vec{B}$ drift with the gradients in $|\vec{B}|$ and $\vec{V}_E$ at the shock front.

In the plasma rest frames time variations in $T_\parallel$ are due to the magnetic mirror force plus the interaction of the $\vec{E} \times \vec{B}$ drift either with temporal and spatial variations in the direction of $\vec{B}$. Time variations in $T_\perp$ are due to the

magnetic mirror force and the interaction of the $\vec{E} \times \vec{B}$ drift with temporal and spatial variations in $\vec{V}_E$, and spatial variations in $|\vec{B}|$.

In the null electric field frame temporal variations in both $T_\parallel$ and $T_\perp$ are due solely to the magnetic mirror force.

2. Calculation Via Transformations

The post encounter pitch angles are derived using the same series of coordinate system transformations utilized in the post shock energy calculations. The post-encounter pitch angle in the particles post encounter plasma rest frame for reflected particles (α_{fR}), transmitted downstream particles (α_{fD}) and transmitted upstream particles (α_{fU}) are given in Equations (21), (22), and (23) respectively.

$$\tan \alpha_{fR} = \frac{S}{2R - \chi} \tag{21}$$

$$\tan \alpha_{fD} = \frac{S\sqrt{N}}{JR - [1 + R(R - 2\chi) - N S^2]^{1/2}} \tag{22}$$

$$\tan \alpha_{fU} = \frac{S N^{-1/2}}{R - [1 + JR(JR - 2\chi) - N^{-1} S^2]^{1/2}} \quad . \tag{23}$$

Expanding the radical in (22) and taking the limit as $\psi_1 \to 90°$, gives

$$\tan \alpha_{fD} = \sqrt{N} \tan \alpha_i \quad . \tag{24}$$

The above equations and Equations (6) - (20) are all averaged over a gyrotropic phase angle distribution. The post-encounter pitch angles show that as expected from angular momentum considerations, reflected particles gain energy only in their parallel component and transmitted particles gain energy predominantly in the perpendicular component. Note that in Equation (22) some transmitted downstream particles are directed back towards the shock in the downstream plasma rest frame, i.e.,

$\alpha_{FD} < 90°$. However, no transmitted downstream particle has a sufficiently large parallel speed to overtake the shock.

Equations (21) - (23) are kinematically consistent in that upstream particles reflected (transmitted) by the shock always outrun the shock (always are left behind by the shock). Likewise downstream particles transmitted by the shock always outrun the shock.

Equations (11) - (24) give the post-encounter energies and pitch angles in the plasma rest frame. Since all observations are made in the spacecraft rest frame, these equations must be transformed into the spacecraft rest frame.

The expression for post-encounter $\Delta T/T_i$ and α_f in that frame can be obtained by making the following substitutions

$$R \to R + (\vec{V}_{w1} \cdot n)\cos\psi_1 |\vec{V}_i|^{-1}$$

$$J\,R \to J\,R + (\vec{V}_{w2} \cdot n)\frac{\cos\psi_1}{N} |\vec{V}_i|^{-1}$$

where $\vec{V}_{w1}$ ($\vec{V}_{w2}$) is the solar wind velocity upstream (downstream) of shock in the spacecraft rest frame.

C. Particle-Shock Interaction Time

The particle-shock interaction time can be estimated by calculating the time it takes for a particle to be mirrored or transmitted in the null electric field frame. In this frame the time rate of change of the particles parallel velocity $V'_{\parallel}$ is given approximately by

$$m\frac{dV'_{\parallel}}{dt} \simeq \frac{mV'^2_{\perp}}{2|B|} V |\vec{B}| \left(\frac{\cos\psi_1 + \cos\psi_2}{2}\right) \tag{25}$$

where $V'_\perp$ is the particle gyration speed in the null electric field frame, and $V'_\parallel$ is positive when the particle is directed towards the upstream region.

The effective $\nabla|\vec{B}|$ experience by the particle at the shock discontinuity is approximately the change in $|\vec{B}|$ divided by twice the particle gyroradius

$$\nabla |\vec{B}| \sim \frac{|\vec{B}_1|(N-1)}{2mV'_\perp} q|\vec{B}| \tag{26}$$

Substituting equation (25) into (26) gives:

$$\frac{dV'_\parallel}{dt} \sim \frac{V'_\perp}{8} \frac{|\vec{B}_1|(N-1)}{1} q \left(\cos \psi_1 + \frac{\cos \psi_1}{N}\right)$$

where from the continuity of the normal component of $\vec{B}$ across the shock $\cos \psi_2 = N^{-1} \cos \psi_1$. In the null electric field frame $V'^2_\parallel + V'^2_\perp =$ constant $= V'^2$ which gives

$$\frac{dV'_\parallel}{\sqrt{V'^2 - V'^2_\parallel}} \sim \frac{\Omega_1 (N-1)}{8} \cos \psi_1 \left(1 + \frac{1}{N}\right) dt \tag{27}$$

where $\Omega_1 = q|\vec{B}_1|m^{-1}$.

Integrating equation (27) gives

$$\alpha' \sim \alpha'_i - \frac{\Omega_1(N-1)}{8} \cos \psi_1 \left(1 + \frac{1}{N}\right) t$$

where $\alpha' = \cos^{-1} V'_\parallel/V'$ and α'_i is the initial value of the pitch angle in the null electric field frame.

Using the fact that the pre- and post-shock values of V' are equal for reflected particles, and that the post reflection value of $\alpha' = \pi - \alpha'_i$, the shock interaction time for a reflected particle t_R is given approximately by

$$t_R \sim \frac{8\ N \sec \psi_1}{\Omega_1 (N^2 - 1)} (2\alpha'_i - \pi) \ . \tag{28}$$

The relationship between α'_i and the initial pitch angle in the upstream plasma rest frame α_i is

$$\cos \alpha'_i = (\cos \alpha_i - R)\ (1 - 2R \cos \alpha_i + R^2)^{-1/2} \ .$$

Equation (28) above shows that t_R is proportional to the particle's mass to charge ratio m/q. This result is independent of the assumption made in Equations (25) and (26). It comes from the fact that in the dimensionless form of the Lorentz force equation the dimensionless unit of time is proportional to m/q. For a particle that is transmitted downstream the post transmission value of $\alpha' = \sin^{-1}(\sqrt{N} \sin \alpha'_i)$ and the particle shock interaction time t_{TD} for such particles is approximately

$$t_{TD} \sim \frac{8\ N \sec \psi_1}{\Omega_1 (N^2 - 1)} [\sin^{-1} (\sqrt{N} \sin \alpha'_i) - \alpha'_i] \tag{29}$$

For a particle that is transmitted upstream, the sign of the right hand term in equation (25) is positive, the post transmission value of $\alpha' = \sin^{-1} (N^{1/2} \sin \alpha'_i)$ and the shock interaction time t_{TU} for such a particle is approximately

$$t_{TU} \sim \frac{8\ N \sec \psi_1}{\Omega_1 (N^2 - 1)} [\sin^{-1} (N^{-1/2} \sin \alpha'_i) - \alpha'_i] \ . \tag{30}$$

Equations (28) - (30) are not valid for shocks in which $V_{ix} \tan \psi_1 - |\vec{V}_s \times \hat{n} >|$ is greater than the speed of light, as there is no inertial frame in which the shock induced $\vec{E} = 0$. For this $\psi \cong 90°$ situation the interaction time can be estimated from Equation (31),

$$\Delta T = \vec{J} \cdot \vec{E}\ t_\perp \tag{31}$$

where ΔT is the particle fractional change in kinetic energy = $(N + 1)\ 0.5\ mV^2$, $\vec{J}$ is the grad B drift induced current $|\vec{J}| = qmV^2 \nabla |\vec{B}| (2q|\vec{B}|^{2-1})$, $V_\perp$ is the particle gyration speed in its guiding center rest frame, and $t_\perp$ is the shock interaction time for a perpendicular shock. Combining the above terms gives,

$$t_\perp \sim \Omega_1^{-1}(N + 1)V_\perp V_{1x}^{-1} \quad . \qquad (32).$$

V. NUMERICAL SIMULATION RESULTS

A. Test of the Equality of Pre- and Post-Encounter μ Assumption

In order to test the assumption that the pre- and post-encounter values of μ are equal in the null electric field frame, it is necessary to follow particles' trajectories throughout the shock interaction in that frame and compare the ensemble average of the post-interaction value of μ with the initial value.

Since the particles' trajectory in the null electric field frame (and shock rest frame) can be expressed in terms of analytical functions, numerical integration techniques are not needed. The procedure is to choose the initial position (x_i, y_i, z_i) and velocity $(\dot{x}_i, \dot{y}_i, \dot{z}_i)$ of the particle and time step size Δt and then compute the position and velocity of the particle at time $t_1 = \Delta t$. The position and velocity at time t_1 are then used as initial conditions to calculate the position and velocity at time $t_2 = 2\Delta t$, and so on.

The algorithms used to compute the particles' position and velocity are theoretically exact and in practice accurate to the single precision (11 digit) accuracy of a Control Data 3800 computer on which the calculations were carried out. Positional and velocity errors occur if, during a step, the particle crosses the shock. The errors occur because gyroradius, gyrofrequency and drift velocity do not change during a step but do change across the shock. This error is minimized by using an iteration process to calculate the time the particles cross the shock and changing the step size accordingly so that the particle does not cross the shock but "ends up" at the shock surface and then starts the next step with the appropriate gyroradius, gyrofrequency, and drift velocity.

That the pre- and post-encounter value of μ for a particle which is transmitted or reflected by a fast move shock wave should be equal is not self-evident.

According to adiabatic theory of charged particle motion [Northrop, 1963], μ averaged over a gyroperiod is conserved for static fields if

$$L \gg R_g \tag{33}$$

where L is the scale length over which the magnitude of the magnetic field changes and R_g is the particle gyroradius. In the shocks to be considered, $|\vec{B}|$ changes discontinuously by a factor of 2 or more and clearly Equation (33) is violated. However, Pesses [1981] has shown that for perpendicular shocks ($\psi_1 = 90°$), the equality of the pre- and post-encounter values of μ is due to the continuity of the flux of particle plus field angular momentum through the shock.

The equality of the pre- and post-encounter μ assumption was tested by calculating $\mu_{final}/\mu_{initial}$ for different values of the particle speed and pitch angle in the null electric field frame.

The results for particles initially upstream for the case N = 2, $\psi_1 = 89°$ and $|\vec{V}_{i1}| = 10\ V_{1x}$ are presented in Table 1. Column 1 presents the initial pitch angle where in this table, and this table only, , particles with $\alpha'_1 < 90°$ are directed towards the shock. Column 2 gives the gyrophase averaged value of the ratio of the post-encounter value of μ to the pre-interaction value (μ_f/μ_i). Column 3 presents the gyrophase averaged fractional change in kinetic. Column 4 (5) gives the maximum (minimum) value of μ_f/μ_i for each pitch angle group. Column 6 gives the range of the number of shock crossings. Column 7 tells whether particles within that pitch angle group were transmitted (T) or reflected (R).

As $\vec{E} = 0$ in the frame in which the simulation is carried out, the nonzero values of $\Delta T/T_i$ indicate that computer round off errors are occurring and/or the interation process to calculate the shock crossing time is not converging

fast enough. However, the errors are only 1 part in 10^6 even after 174 shock crossings and give confidence to the numerical technique used. Column 2 shows the precision with which the initial and final gyrophase-averaged μ are equal increases with increasing α_i', ranging from a difference of 8% at $\alpha_i' = 10°$ to 0.0008% at $\alpha_i' = 81°$. Columns 4 and 5 show the the precision with which an individual particle's pre- and post-shock μ are equal increases with increasing α_i', with lower limits ranging from 68% at $\alpha_i' = 1°$ to 0.01% at $\alpha_i' = 81°$. Column 7 shows that test particles with $\alpha_i' < 41°$ ($> 51°$) are transmitted (reflected). The latter result is consistent with the reflection/transmission criteria discussed in section IV A2 which predicts that for a strength two shock upstream particles with $\alpha_1' < (>)\ 45°$ are transmitted (reflected).

The equality of initial and final μ assumption for particles originating in the downstream, high $|\vec{B}|$ region was also tested. As in the initially upstream case, the pre- and post-shock values of μ were found to be equal to $\sim 1\%$ for $\alpha_i' = 11°$ to $\sim .001\%$ for $\alpha_i' = 81°$. Runs were also made for both upstream and downstream particles with $V_i = 20$, $30\ V_{1x}$ and with $N = 4$ with similar results.

B. Comparison of Analytical Model Predictions of Energy Gains with Numerical Simulations

1. Perpendicular Shocks

Equation (14) predicts that in the limit $\psi_1 \to 90°$ (a perpendicular shock) $\Delta T/T_i = (N - 1) \sin^2 \alpha_i$. This means that averaged over phase angle $\mu_f/\mu_i = 1$. Numerical simulations of the interaction of charged particles with perpendicular shocks have been carried out previously. Parker [1958] found that averaging over entrance gyrophase the pre- and post-shock valus of μ are equal for

infinitesimally thin fast-mode perpendicular shocks. Chen and Armstrong [1972] and Pesses [1979], with more extensive studies, confirmed Parker's [1958] results. A typical particle trajectory in the x - y plane of a perpendicular shock is shown in Figure 2 of Pesses [1981].

2. Oblique Shocks

Numerical studies of the interaction of charged particles with oblique shocks have been done by Hudson [1965], Quenby and Webb [1973], Chen [1975], Pesses [1979], Terasawa [1979] and Decker [1981]. The first two papers are concerned with the conditions for reflection and transmission. Chen [1975] made a detailed study of the post-interaction energy and pitch angle distribution as a function of N, ψ_1 and $V_{1x}V_i^{-1}$. Chen also considered the effects of charged particle scattering by magnetic field irregularities. Terasawa [1979] did a study similar to Chen [1975] and also considered the effects of a finite shock thickness.

The predictions of the analytical model of shock acceleration derived in Section IV have been compared with results from independent numerical simulations by Pesses [1979] which uses the same particle following technique described in Section V A.

The particle's initial position, velocity, pitch angle, and phase angle are specified in a plasma rest frame and then transformed to the shock rest frame. After the particle-shock interaction is completed, the particle velocity vector is transformed back to the appropriate plasma rest frame. The results presented are averaged over initial and final gyrophase.

In Figure 3, Equations (12) and (11) are compared to the numerical simulations results for the case $\psi_1 = 84°$, N = 2 and $V_i = 40\ V_{1x}$. The vertical axis gives $\Delta T/T_i$, the horizontal axis α_i. The portion of the curve labeled R

(T) [N] is for reflected (transmitted) [noninteracting] particles. The analytical and numerical values are in excellent agreement. Pesses [1979] has shown the agreement between the predictions of the analytical equations presented in Section IV of this paper and the numerical simulations for final pitch angles and reflection, transmission and noninteracting coefficients are also excellent.

C. Acceleration Time

Equations (28) - (31) show that the particle's acceleration time in the shock is proportional to its gyroperiod. Hence the acceleration time is inversely proportional to the magnetic field strength and proportional to the particle mass to charge ratio m/q.

To check the accuracy of the analytical expressions for acceleration time (Equations 28-31) the particle-shock interaction time is calculated numerically. The partial shock interact time is defined as the time between the particles first and last crossing of the shock front. The time as a function of the particle gyrofrequency in the upstream region Ω_1^{-1} is calculated using the same numerical procedure as described above for the μ_f/μ_i; and $\Delta T/T_i$ calculations. An example of the agreement between one numerical and analytical acceleration times is given in Figure 3. The numerical (solid circles) and analytical calculated (solid curve) value of t_R and t_{rD} as a function of α_i are compared for the case; $\psi_1 = 82°$, $N = 2$, and $R = 1$. The agreement between the analytically and numerically calculated acceleration time is very good for transmitted particles, and fair for reflected particles.

The perpendicular shock interaction times predictd by Equation (32) are also consistent with those calculated numerically by Pesses [1979]. For example, for $N = 2$ and $V_{\perp i} V_{1x}^{-1} = 20$ Pesses [1979] finds that $t_\perp = 42\ \Omega_1^{-1}$, while Equation (32) predicts $t_\perp \sim 40\ \Omega_1^{-1}$.

VI. CONCLUSION

This paper has dealt primarily with the physics and calculations of the energy gain of energetic particles that are reflected or transmitted by magnetosonic fast-mode shock waves. For a typical interplanetary shock of magnetic strength N = 2 the maximum increase in a particle energy from one shock encounter is a factor of 5.85. For an ion with an initial energy of 30 keV/nuc to end up with 10 MeV/nuc at least four shock encounters are needed. Clearly, in order to understand interplanetary shock acceleration phenomena, which routinely result in 10 MeV protons, it is necessary to extend the single encounter model in this paper to a multiple encounter model. Such a model is presented Paper II.

ACKNOWLEDGMENTS

I am grateful to J.A. Van Allen for general advice and support. I have benefitted from conversations with R. Decker, D. Eichler, M. Forman, M. Lee and C. Goertz.

This work was supported at the University of Iowa by Contract NAS2-GS53 with the Ames Research Center/NASA and by the U.S. Office of Naval Research and at the Goddard Space Flight Center/NASA by the Laboratory for Astronomy and Solar Physics. The author is a National Academy of Sciences' National Research Council Resident Research Associate at GSFC.

REFERENCES

Alekseyev, I.I., and A.P. Kropotkin, Passage of energetic particles through a magnetohydrodynamic discontinuity surface, Geomagn. and Aeronomy, 10, 755-763, 1970.

Armstrong, T.P., G. Chen, E.G. Sarris, and S.M. Krimigis, Acceleration and modulation of electrons and ions by propagating interplanetary shocks, in Study of Traveling Interplanetary Phenomena, edited by M.A. Shea, D.F. Smart, and S.T. Wu, pp. 367-389, D. Reiderl, Dordrecht-Holland, 1977.

Axford, W.I., and G.C. Reid, Increases in intensity of solar cosmic rays before sudden commencements of geomagnetic storms, J. Geophys. Res., 68, 1973-1803 1963.

Axford, W.I., E. Leer, and G. Skardon, Proc. 15th International Cosmic Ray Conference, Plovdiv, 2, 273, 1977.

Bell, A.R., The acceleration of cosmic rays in shock fronts, Mon. Nat. R. Astr. Soc., 182, 147-156, 1978.

Chen, G., Numerical simulation of the interaction of charged particles with oblique magnetohydrodynamic shocks, Ph.D. thesis, University of Kansas, Lawrence, 1975.

Chen, G., and T.P. Armstrong, Particle acceleration in the interplanetary medium: I. Numerical simulation of the motions of charged particles near interplanetary shock waves, partial summary of a contribution to Panel Presentation 5 of the Conference on Solar Terrestrial Relations, Calgary, August 28 - September 1, 1972.

Decker, R.B., The modulation of low energy proton distributions by propagating interplanetary shock waves: A numerical simulation, J. Geophys. Res., 86, 4537, 1981.

Fermi, E., On the origin of the cosmic radiation, Phys. Rev., 75, 1169-1174, 1949.

Fink, L.A., Increase in the low-energy cosmic ray intensity at the front of propagating interplanetary shock waves, J. Geophys. Res., 76, 1662-1672, 1971.

Fisk, L.A., and M.A. Lee, Shock acceleration of energetic particles in corotating interaction regions, Astrophys. J., 237, 620-624, 1980.

Hudson, P.D., Reflection of charged particles by plasma shocks, Mon. Not. R. Astron. Soc., 131, 23-25, 1965.

Northrop, T., Adiabatic charged-particle motion, Rev. Geophys., 1, 283-304, 1963.

Palmer, I.D., and Gosling, J.T., Shock-associated energetic proton events at large heliocentric distances, J. Geophys. Res., 83, 2037-2045, 1978.

Parker, E.N., unpublished manuscript, 1958.

Parker, E.N., Interplanetary dynamical processes, Interscience, New York, 1963.

Pesses, M.E., On the acceleration of energetic protons by interplanetary shock waves, Ph. D. thesis, University of Iowa, Iowa City, 1979.

Pesses, M.E., On the conservation of the first adiabatic invariant in perpendicular shocks, J. Geophys. Res., 86, 150-152, 1981.

Pesses, M.E., B.T. Tsurutani, J.A. Van Allen, and E.J. Smith, Acceleration of energetic protons by interplanetary shocks, J. Geophys. Res., 84, 7297-7301, 1979.

Quenby, J.J., and S. Webb, Numerical studies of the interaction of energetic particles with interplanetary field discontinuities, Proc. 13th International Cosmic Ray Conference, 2, 1343-1347, 1973.

Sarris, E.T., Effects of interplanetary shock waves on energetic charged particles, Ph.D. thesis, University of Iowa, Iowa City, 1973.

PRECEDING PAGE BLANK NOT FILMED

FIGURE CAPTIONS

Figure 1: Shock geometry in the shock rest frame.

Figure 2:

a and b: Graphic view of acceleration process at shock front in the upstream (a) and downstream (b) plasma rest frames.

Figure 3: The dependence of $\Delta T/T_i$ on α_i, for $\psi_1 = 84°$, $N = 2$, $V_i = 40\ V_{1x}$. Model predictions shown as solid lines, numerical results shown as solid circles. R,T and N stands for reflected upstream, transmitted downstream and noninteracting particles, respectively.

Figure 4: The dependence of acceleration time on α_i for $\psi_1 = 82°$, $N = 2$, and $R = 1$. Model predictions shown as solid lines, numerical simulation results shown as solid circles. τ_R, τ_{TD} stands for reflected upstream, transmitted downstream particles, respectively.

Table 1

Conservation of First Adiabatic Invarient

$N = 2$ $\psi_1 = 89°$ $\psi_2 = 89.5°$						
α	$\langle\mu_f/\mu_i\rangle$	$\Delta T/T_i$	$\mu_f/\mu_i max$	$\mu_f/\mu_i min$	# Crossings	R/T
1	1.08391	1.096×10^{-6}	1.68348	0.390064	1 or 3	T
11	1.00122	1.366×10^{-7}	1.02527	0.968477	11 or 12	T
21	0.999978	2.565×10^{-7}	1.00765	0.986034	23 or 25	T
31	0.999954	3.738×10^{-7}	1.00233	0.993105	41 or 43	T
41	0.999958	5.431×10^{-7}	1.00191	0.995753	73 or 75	T
51	0.999283	9.238×10^{-7}	1.00104	0.997076	174	R
61	1.00005	1.304×10^{-6}	1.00196	0.998086	132 or 134	R
71	1.00002	1.248×10^{-6}	1.00059	0.999567	104 or 106	R
81	0.999992	1.199×10^{-6}	1.00009	0.999891	78	R

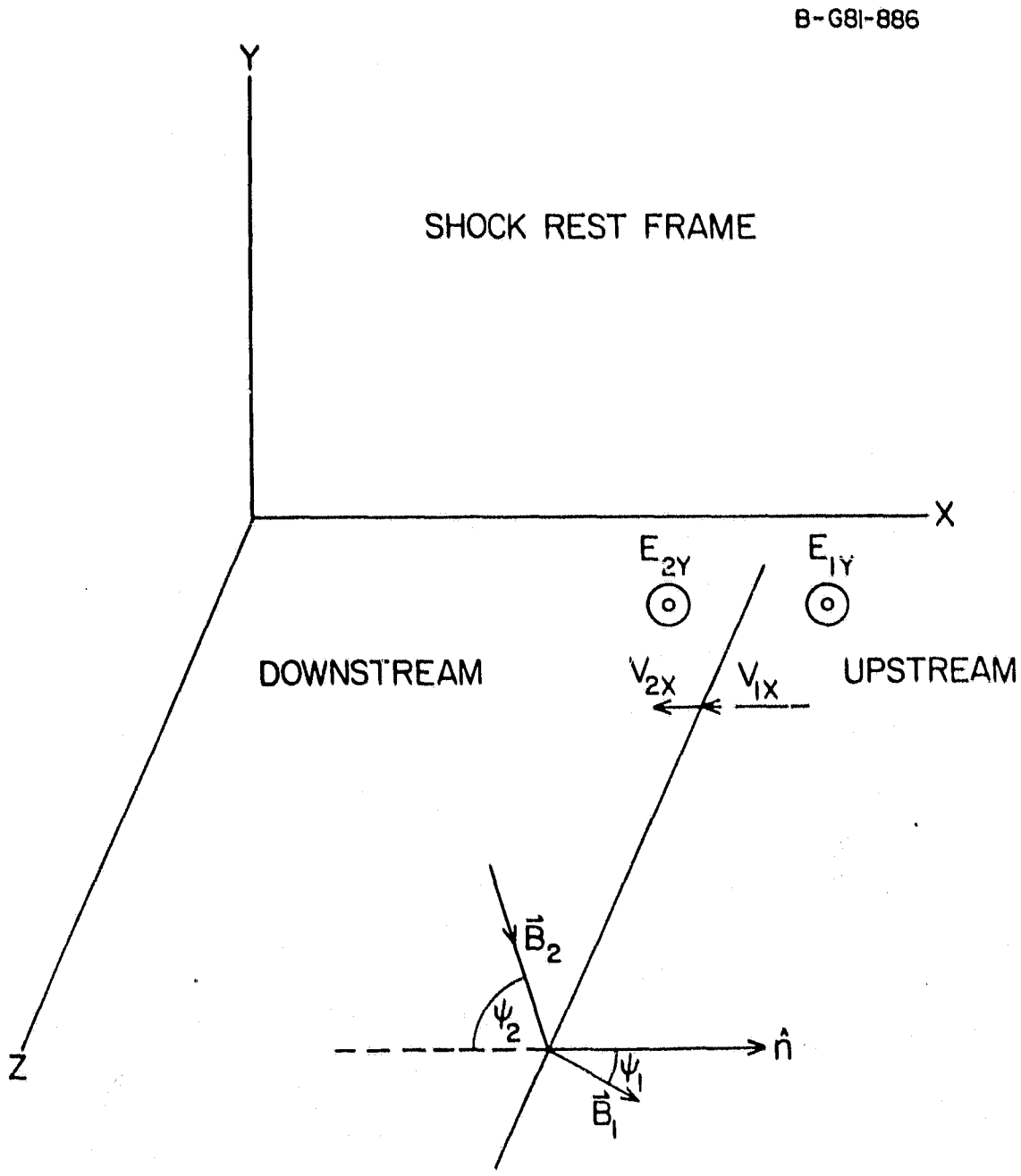
B-G81-886
Y
SHOCK REST FRAME
X
E_{2Y}
E_{1Y}
DOWNSTREAM
V_{2X}
V_{1X}
UPSTREAM
$\vec{B}_2$
ψ_2
$\hat{n}$
ψ_1
$\vec{B}_1$
Z

Figure 1

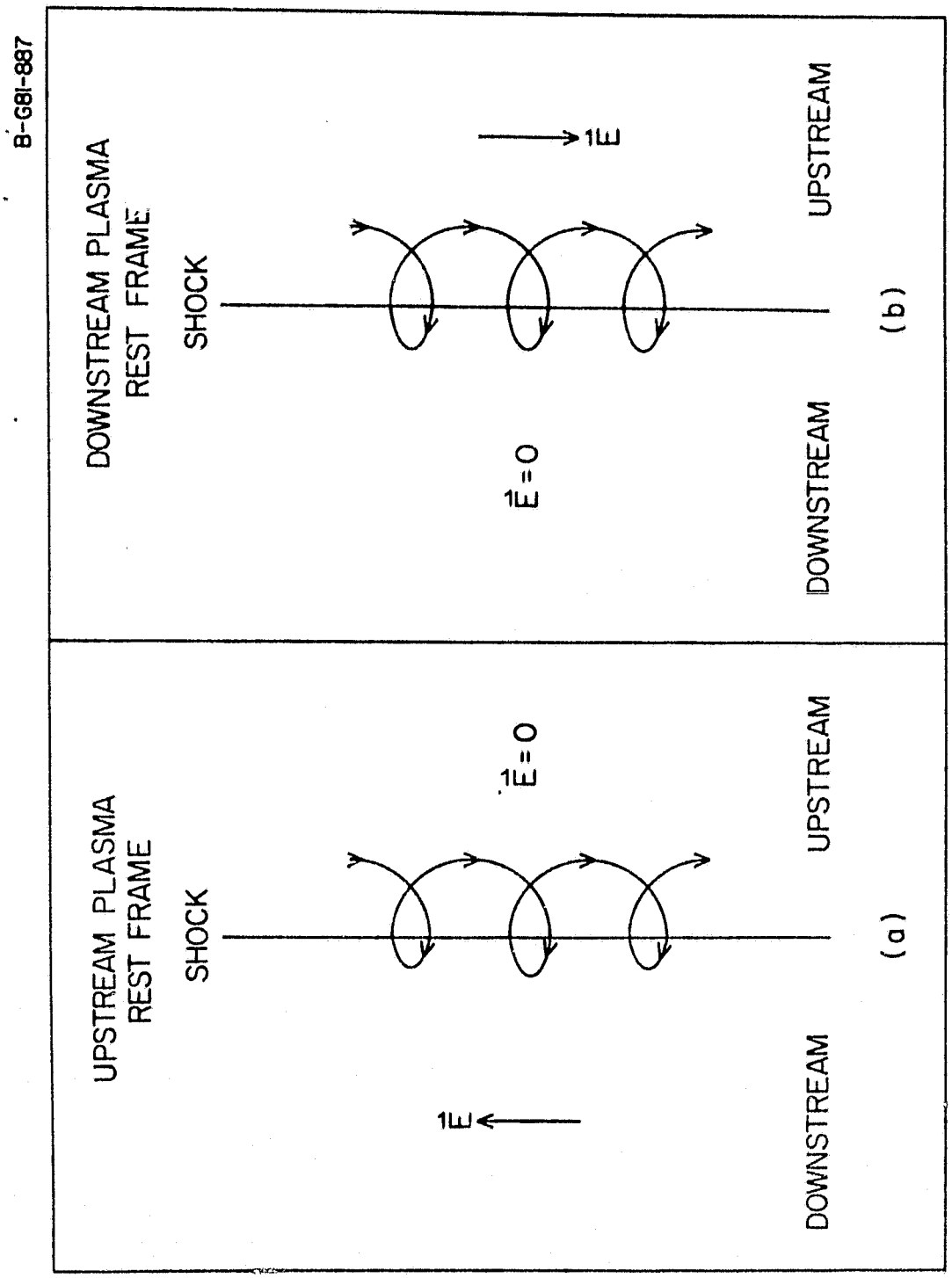
B-G81-887
DOWNSTREAM PLASMA
REST FRAME
SHOCK
1E
1E=0
UPSTREAM
DOWNSTREAM
(b)
UPSTREAM PLASMA
REST FRAME
SHOCK
1E=0
1E
UPSTREAM
DOWNSTREAM
(a)

Figure 2

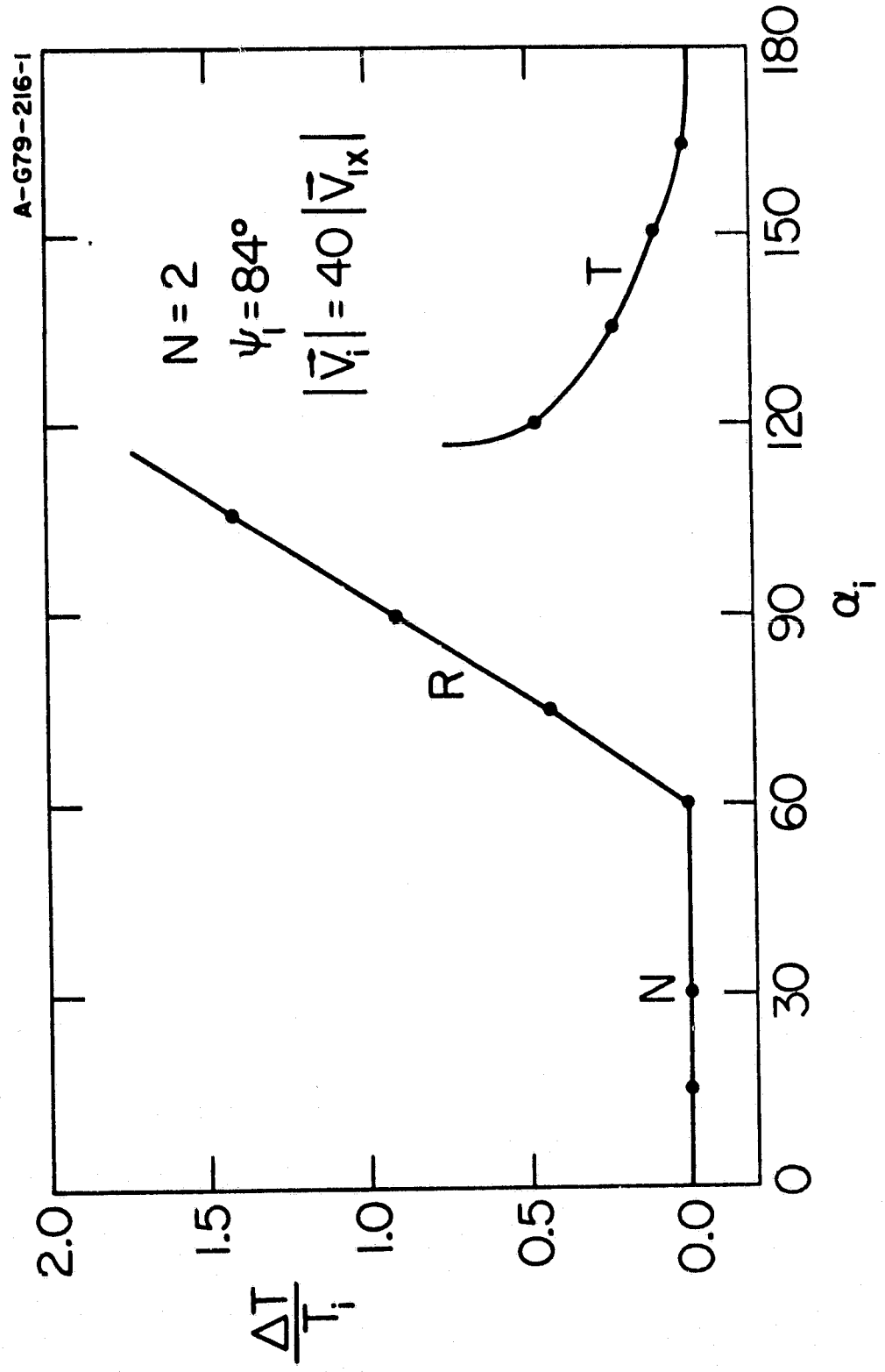
A-G79-216-1
N = 2
$\psi_1 = 84°$
$|\vec{V}_i| = 40\,|\vec{V}_{1x}|$
R
N
T
$\frac{\Delta T}{T_i}$
2.0
1.5
1.0
0.5
0.0
0
30
60
90
120
150
180
α_i

Figure 3

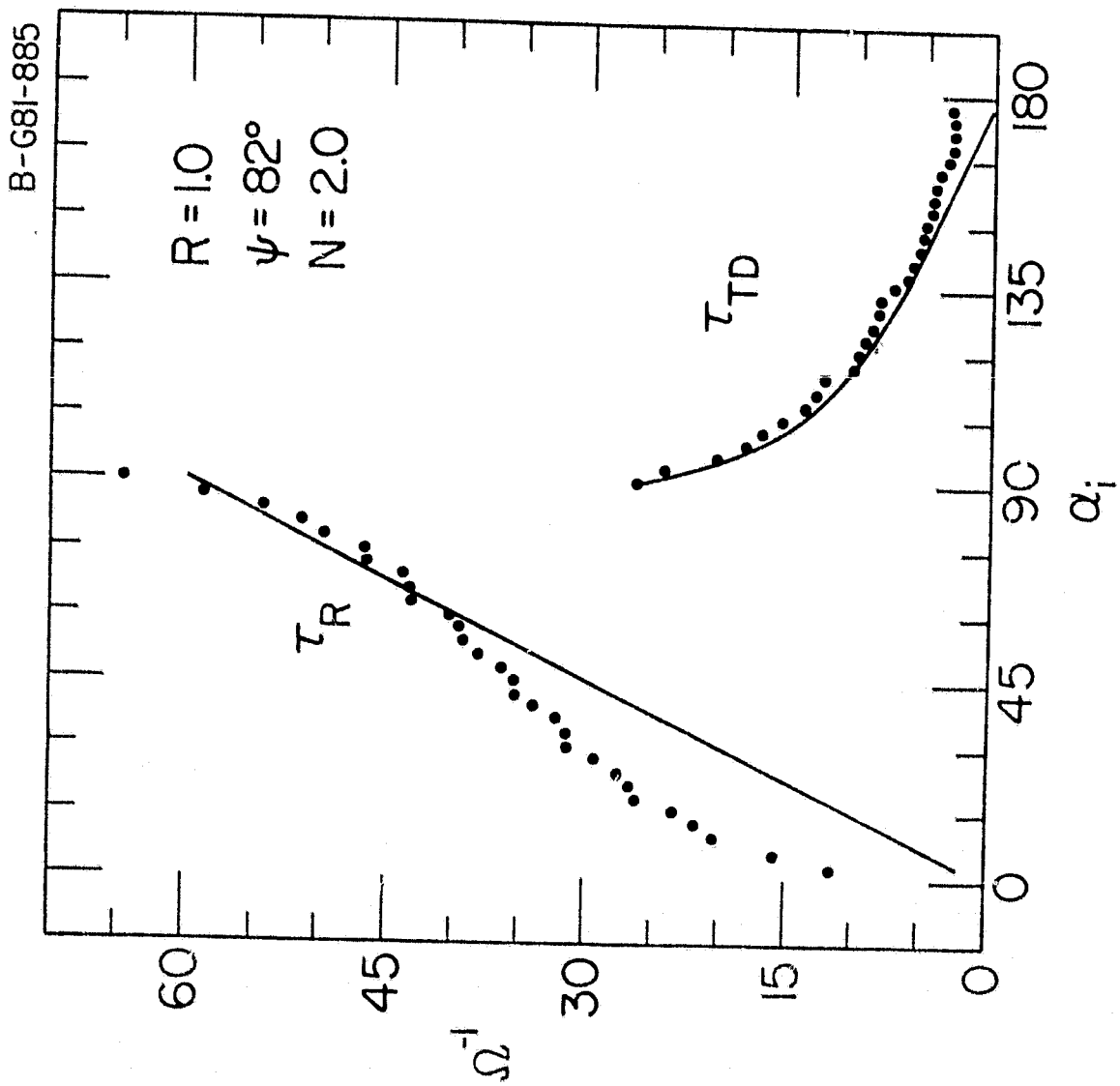

Figure 4